

DCF Throughput Analysis of IEEE 802.11a/g/n-based Mobile LAN over Correlated Fading Channel

Ha Cheol Lee

Dept. of Information and Telecom. Eng. Yuhan University
185-34 Goean-Dong, Sosa-Gu, Bucheon City, Gyeonggi-Do, Korea
hclee@yuhan.ac.kr

Abstract: This paper explores a MAC (Medium Access Control) layer throughput with DCF (Distributed Coordination Function) protocol in the IEEE 802.11a/g/n-based mobile LAN. It is evaluated in Rayleigh fading wireless channel, using theoretical analysis method. The DCF throughput performance is analyzed by using the number of stations with both variable payload size and mobile speed on the condition that fading margin and transmission probability are fixed. In the IEEE 802.11n, A-MSDU (MAC Service Data Unit Aggregation) scheme is considered and number of subframe is used as the variable parameter. It is identified that MAC efficiency of IEEE 802.11n is the best out of four schemes.

Keywords: Mobile LAN, MAC, Throughput, CSMA/CA, DCF, IEEE 802.11a/g/n.

1. Introduction

Over the past few years, mobile networks have emerged as a promising approach for future mobile IP applications. With limited frequency resources, designing an effective MAC protocol is a hot challenge. IEEE 802.11b/g/a/n networks are currently the most popular wireless LAN products on the market [1]-[3]. The conventional IEEE 802.11b and 802.11g/a specification provide up to 11 and 54 Mbps data rates, respectively. However, the MAC protocol that they are based upon is the same and employs a CSMA/CA (Carrier Sense Multiple Access/Collision Avoidance) protocol with binary exponential back-off. IEEE 802.11 DCF is the de facto MAC protocol for wireless LAN because of its simplicity and robustness [1]. Therefore, considerable research efforts have been put on the investigation of the DCF performance over wireless LAN [4]-[7]. With the successful deployment of IEEE 802.11a/b/g wireless LAN and the increasing demand for real-time applications over wireless, the IEEE 802.11n Working Group standardized a new MAC and PHY (Physical) Layer specification to increase the bit rate to be up to 600 Mbps [8],[9]. The throughput performance at the MAC layer can be improved by aggregating several frames before transmission [10]. Frame aggregation not only reduces the transmission time for preamble and frame headers, but also reduces the waiting time during CSMA/CA random backoff period for successive frame transmissions. The frame aggregation can be performed within different sub-layers. In 802.11n, frame aggregation can be performed either by A-MPDU (MAC Protocol Data Unit Aggregation) or A-MSDU (MAC Service Data Unit Aggregation). Although frame aggregation can increase the throughput at the MAC layer under ideal channel conditions, a larger aggregated frame will cause each station to wait longer before its next chance for channel access. Under error-prone channels, corrupting a large aggregated frame may waste a long period of channel time and lead to a lower MAC efficiency [11]-[13]. On the other hand, wireless LAN mobile stations that are defined as the stations that access the LAN while in motion are considered in this paper [7]. The previous paper analyzed the IEEE 802.11b/g/n MAC performance for wireless LAN with fixed stations, not for wireless LAN with mobile stations [4]-[7],[10]-[13]. On the contrary, reference 7 and 14 analyzed the MAC performance for IEEE 802.11 wireless LAN with mobile stations, but considered only IEEE 802.11 and 802.11g/a wireless LAN specification. So, this paper extends the previous researches and

analyzes the IEEE 802.11n MAC performance for wireless LAN with mobile stations. In other words, we will present the analytical evaluation of saturation throughput with bit errors appearing in the transmitting channel. IEEE 802.11g/a/n PHY and MAC layer focused in this paper are reviewed and frame error rate of mobile wireless channel is derived in section 2. The DCF saturation throughput is theoretically derived in section 3 and numerical results are analyzed in section 4. Finally, it is concluded with section 5.

2. Wireless access architecture

A. 802.11a/g/n-based wireless access architecture

Figure 1 shows ad-hoc mode operation in the mobile LAN. The protocols of the various layers are called the protocol stack. The TCP/IP protocol stack consists of five layers: the physical, data link, network, transport and application layers. 802.11 of Figure 1 means physical layer and data link layer which consists of MAC and LLC (Logical Link Control) sub-layers. And this paper is focused on physical layer and MAC sublayer. An ad-hoc network might be formed when people with laptops get together and want to exchange data in the absence of a centralized AP (Access Point).

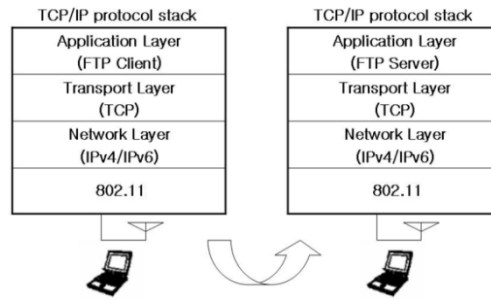


Figure 1. Ad-hoc mode operation in the mobile LAN

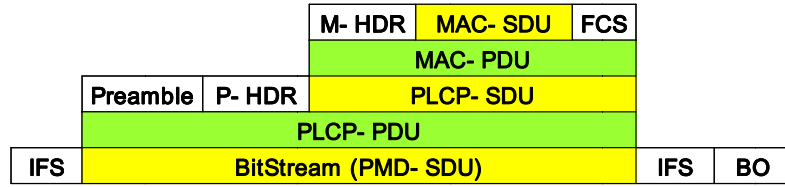
Table 1. Shows IEEE 802.11n OFDM parameter compared to IEEE 802.11a/g.

Standards	IEEE 802.11a/g	IEEE 802.11n	
		Mandatory	Optional
Maximum transmission rate (Mbps)	54	130	600
Bandwidth(MHz)	20	20	40
FFT size	64	64	128
Number of subcarrier (data + pilot)	52 (48+4)	56 (52+4)	114 (108+6)
Multi-antenna scheme	signal antenna	2 Tx MIMO	3,4 Tx MIMO Tx Beam forming STBC
Channel coding	Convolutional code (1/2, 2/3, 3/4)	Convolutional code (1/2, 2/3, 3/4, 5/6)	LDPC (1/2, 2/3, 3/4, 5/6)
Modulation	BPSK, QPSK, 16-QAM, 64-QAM		
Spatial stream	1	1 ~ 2	1 ~ 4
Guard interval(ns)	800	800	400
Subcarrier interval	312.5 KHz	312.5 KHz	312.5 KHz
FFT period	3.2 μ s	3.2 μ s	3.2 μ s
Symbol period	4 μ s	4 μ s	4 μ s

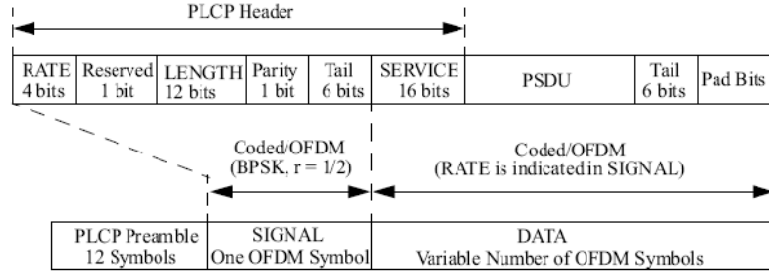
B. 802.11a/g PHY/MAC layer

Figure 2 shows the 802.11a/g-based physical and MAC layer protocol stack and typical frame structure focused in this paper. When a higher layer pushes a user packet down to the MAC layer as a MAC-SDU (MSDU), the M-HDR (MAC layer header) and FCS (trailer) are added before and after the MSDU, respectively and form a MPDU (MAC-PDU). The PHY layer is again divided into a PLCP (Physical Layer Convergence Protocol) sub-layer and a PMD (Physical Medium Dependent) sub-layer. Similarly the PLCP preamble and P-HDR (PLCP header) are attached to the MPDU at the PLCP sub-layer. Different IFS (Inter Frame Space)s are added depending on the type of MPDU.

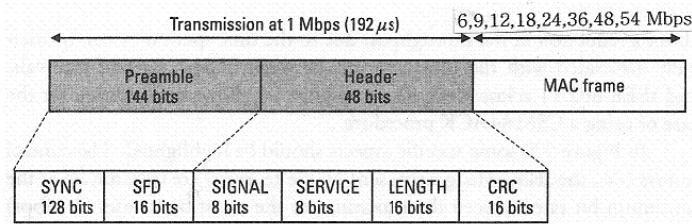
IEEE 802.11a operates in the 5 GHz band and uses OFDM (Orthogonal Frequency Division Multiplexing). The achievable data rates are 6, 9, 12, 18, 24, 36, 48, and 54 Mbps. IEEE 802.11g uses DSSS, OFDM, or both at the 2.4 GHz ISM band to provide high data rates of up to 54 Mbps. IEEE 802.11g device can operate with an IEEE 802.11b device. Combined use of both DSSS and OFDM is achieved through the provision of four different physical layers. The four different physical layers defined in the IEEE 802.11g standards are ERP-DSSS/CCK, ERP-OFDM, ERP-DSSS/PBCC and DSSS-OFDM. The standards that support the highest data rate of 54 Mbps are ERP-OFDM and DSSS-OFDM. ERP-OFDM is a new physical layer in IEEE 802.11g and OFDM is used to provide IEEE 802.11a data rates at the 2.4 GHz band. DSSS-OFDM is a new physical layer that uses a hybrid combination of DSSS and OFDM. The packet physical header is transmitted using DSSS, while the packet payload is transmitted using OFDM. Figure 3 shows basic access scheme of CSMA/CA mechanism. The SIFS (Short Inter-Frame Space) and the slot time are determined by the physical layer. DIFS (Distributed Inter-Frame Space) is defined based on the above two intervals.



(a) Protocol stack of physical and MAC layer



(b) 802.11a and 802.11g ERP-OFDM frame



(c) 802.11g DSSS-OFDM frame

Figure 2. Protocol stack and frame structure of IEEE 802.11a/g/-based mobile LAN

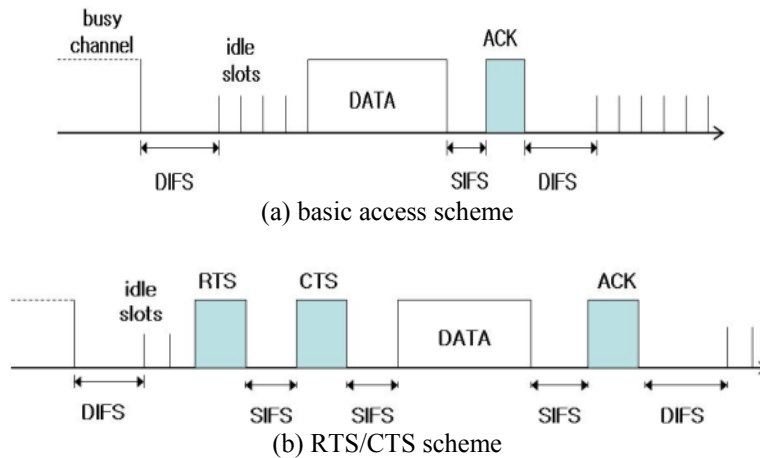


Figure 3. IEEE 802.11g/a DCF channel access mechanism

Table 2. Shows parameters of the IEEE 802.11a physical layer and table 3 shows parameters of the different IEEE 802.11g physical layers

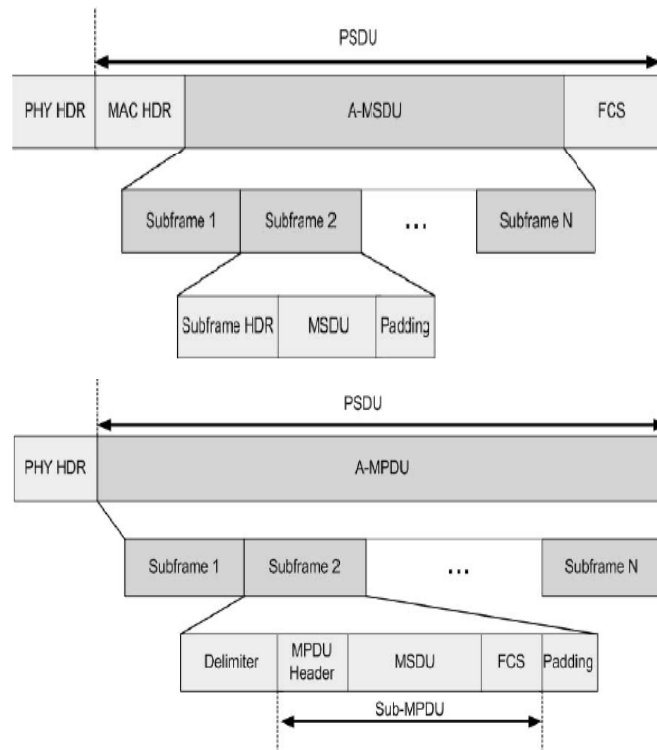
Data Rate (Mbits/sec)	Modulation	Coding Rate (R)	Coding Bits Per Subcarrier (N_{BPSK})	Coded Bits per OFDM symbol (N_{CBPS})	Data Bits Per OFDM Symbol (N_{DBPS})
6	BPSK	1/2	1	48	24
9	BPSK	3/4	1	48	36
12	QPSK	1/2	2	96	48
18	QPSK	3/4	2	96	72
24	16-QAM	1/2	4	192	96
36	16-QAM	3/4	4	192	144
48	64-QAM	2/3	6	288	192
54	64-QAM	3/4	6	288	216

Table 3. Parameters of the different IEEE 802.11g physical layers

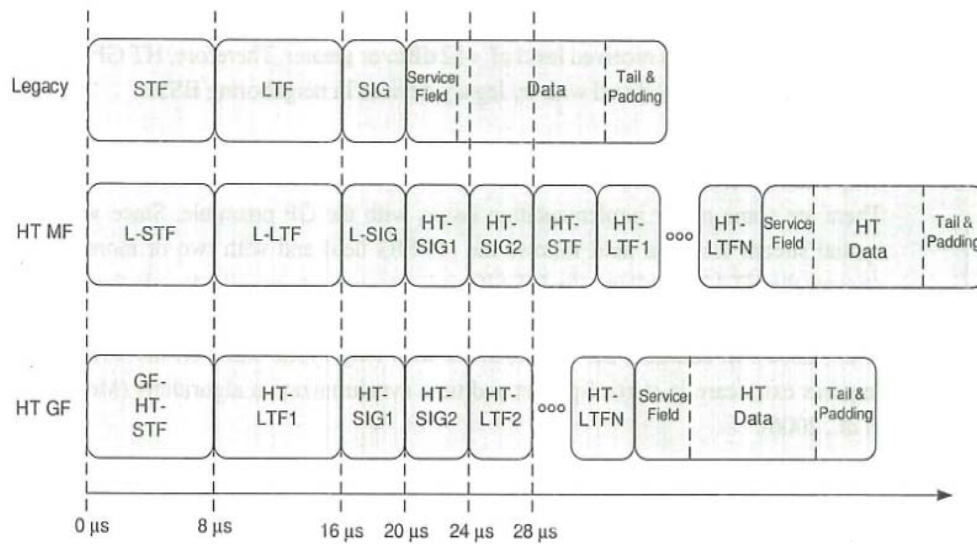
Physical layer	Supported rates (Mb/s)	PLCP preamble + header delay		PLCP preamble + header length	
		Long	Short	Long	Short
ERP-DSSS (mandatory)	1, 2, 5.5, 11	192 μ s	96 μ s	192 bits	120 bits
ERP-OFDM (mandatory)	6, 9, 12, 18, 24, 36, 48, 54	20 μ s		40 bits ¹	
ERP-PBCC (optional)	1, 2, 5.5, 11, 22, 33	192 μ s	96 μ s	192 bits	120 bits
DSSS-OFDM (optional)	6, 9, 12, 18, 24, 36, 48, 54	192 μ s	96 μ s	192 bits	120 bits

C. 802.11n PHY/MAC layer

At the MAC layer, 802.11n use several new MAC, including the frame aggregation, block acknowledgement, and bi-directional data transmission. There are two ways to perform frame aggregation at the MAC layer as shown in Figure 4. The first technique is by concatenating



(a) 802.11n Frame Format for A-MSDU and A-MPDU



(b) Timing of the preamble fields in legacy, MF and GF
Figure 4. Frame structure of IEEE 802.11n-based mobile LAN

several MSDUs (MAC Service Data Units) to form the data payload of a large MPDU (MAC Protocol Data Unit). The PHY header and MAC header, along with the FCS (Frame Check Sequence), are then appended to form the PSDU (Physical Service Data Unit). This technique is known as A-MSDU. The second technique is called A-MPDU. It begins with each MSDU appending with its own MAC header and FCS to form a sub-MPDU. An MPDU delimiter is then inserted before each sub-MPDU. Padding bits are also inserted so that each sub-MPDU is a multiple of 4 bytes in length, which can facilitate subframe delineation at the receiver. Then, all the sub-MPDUs are concatenated to form a large PSDU. Figure 4 also shows timing of the preamble fields in legacy, MF(Mixed Format) and GF (Green Field). At the PHY layer, 802.11n will use MIMO (Multiple-Input Multiple-Output) and OFDM. It supports up to a transmission rate of 600 Mbps and is backward compatible with IEEE 802.11a/b/g. IEEE 802.11n provides support for both 2.4 GHz and 5 GHz frequency bands at the same time. IEEE 802.11n defines implicit and explicit TxBF (Transmit BeamForming) methods and STBC (Space-Time Block Coding), which improves link performance over MIMO with basic SDM (Spatial-Division Multiplexing). It also defines a new optional LDPC (Low Density Parity Check) encoding scheme, which provides better coding performance over the basic convolutional code.

The possible timing sequences for A-MPDU and A-MSDU in the uni-directional transfer case are shown in Figure 5. If RTS/CTS (Request To Send/Clear To Send) is used, the current transmission sequence of RTS–CTS–DATA (Data frame)–ACK (Acknowledgement) only allows the sender to transmit a single data frame. The DATA frame represents either an A-MPDU or an A-MSDU frame. The system time can be broken down into virtual time slots where each slot is the time interval between two consecutive countdown of backoff timers by non-transmitting stations. The IEEE 802.11n also specifies a bi-directional data transfer method. In the bi-directional data transfer method, the receiver may request a *reverse* data transmission in the CTS control frame. The sender can then grant a certain medium time for the receiver on the reverse link. The transmission sequence will then become RTS-CTS-DATAf-DATAr-ACK. This facilitates the transmission of some small feedback packets from the receiver and may also enhance the performance of TCP (Transmission Control Protocol) which requires the transmission of TCP ACK segments. BACK (Block Acknowledgement) can be used to replace the previous ACK frame. The BACK can use a bit map to efficiently acknowledge each individual sub-frame within the aggregated frame.

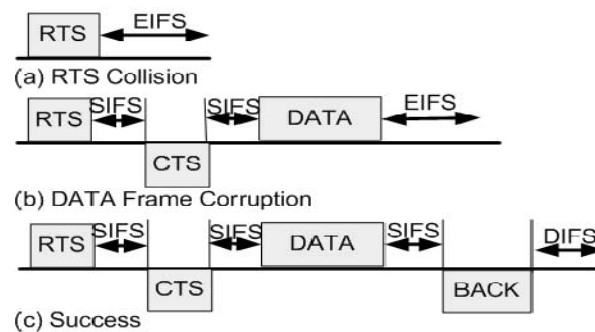


Figure 5. IEEE 802.11n Uni-directional RTS/CTS Access Scheme

Table 4. Parameters of the IEEE 802.11n physical layer, MCS Rates 0-31

MCS Index	Modulation	Coding Rate	Spatial Streams	802.11n Data Rate (Mbps)			
				20-MHz		40-MHz	
				L-GI	S-GI	L-GI	S-GI
0	BPSK	1/2	1	6.5	7.2	13.5	15
1	QPSK	1/2	1	13	14.4	27	30
2	QPSK	3/4	1	19.5	21.7	40.5	45
3	16-QAM	1/2	1	26	28.9	54	60
4	16-QAM	3/4	1	39	43.3	81	90
5	64-QAM	2/3	1	52	57.8	108	120
6	64-QAM	3/4	1	58.5	65	122	135
7	64-QAM	5/6	1	65	72.2	135	150
8	BPSK	1/2	2	13	14.4	27	30
9	QPSK	1/2	2	26	28.9	54	60
10	QPSK	3/4	2	39	43.3	81	90
11	16-QAM	1/2	2	52	57.8	108	120
12	16-QAM	3/4	2	78	86.7	162	180
13	64-QAM	2/3	2	104	116	216	240
14	64-QAM	3/4	2	117	130	243	270
15	64-QAM	5/6	2	130	144	270	300
16	BPSK	1/2	3	19.5	21.7	40.5	45
17	QPSK	1/2	3	39	43.3	81	90
18	QPSK	3/4	3	58.5	65	121.5	135
19	16-QAM	1/2	3	78	86.7	162	180
20	16-QAM	3/4	3	117	130	243	270
21	64-QAM	2/3	3	156	173.3	324	360
22	64-QAM	3/4	3	175.5	195	364.5	405
23	64-QAM	5/6	3	195	216.7	405	450
24	BPSK	1/2	4	26	28.9	54	60
25	QPSK	1/2	4	52	57.8	108	120
26	QPSK	1/2	4	78	86.7	162	180
27	16-QAM	1/2	4	104	115.6	216	240
28	16-QAM	3/4	4	156	173.3	324	360
29	64-QAM	2/3	4	208	231.1	432	480
30	64-QAM	3/4	4	234	260	486	540
31	64-QAM	5/6	4	260	288.9	540	600

D. Frame error rate

Mobile wireless channel is assumed to be flat fading Rayleigh channel with Jake spectrum. The channel is in fading states or inter-fading states by evaluating a certain threshold value of received signal power level. If and only if the whole frame is in inter-fading state, there is the successful frame transmission. If any part of frame is in fading duration, the frame is received in error. In the fading channel fading margin is considered and defined as $\rho = R_{\text{req}}/R_{\text{rms}}$, Where R_{req} is the required received power level and R_{rms} is the mean received power. Generally, the fading duration and inter-fading duration can be taken to be exponentially distributed for $\rho < 10\text{dB}$. With the above assumptions, let T_{pi} be the frame duration, then the frame error rate is given by (1) [7].

$$FER = 1 - \frac{T_i}{T_i + T_f} P(t_i > T_{pi}) \quad (1)$$

Where, t_i is inter-fading duration and t_f is fading duration. T_i is the mean value of the random variable t_i and T_f is the mean value of the random variable t_f . $P(t_i > T_{pi})$ is the probability that inter-fading duration lasts longer than T_{pi} . Since exponential distribution is assumed for t_i , $P(t_i > T_{pi}) = \exp(-\frac{T_{pi}}{T_i})$. For Rayleigh fading channel, the average fading duration is given by (2).

$$T_i = \frac{\exp(\rho) - 1}{fd\sqrt{2\pi\rho}} \quad (2)$$

$T_i + T_f$ is $\frac{1}{N_f}$, where N_f is the level crossing rate, which is given by $fd\sqrt{2\pi\rho} \exp(-\rho)$. f_d

is the maximum Doppler frequency and evaluated as $\frac{v}{\lambda}$. v is the mobile speed and λ is wavelength. Frame error rate can be expressed by (3).

$$FER = 1 - \exp(-\rho - f_d\sqrt{2\pi\rho} T_{pi}) \quad (3)$$

Equation (3) shows that frame error rate is determined by fading margin, maximum Doppler frequency and frame duration. Since fading margin and maximum Doppler frequency are hard to dynamically control, the only controllable parameter is frame duration to get required frame error rate. For the RTS/CTS access mode, the frame duration T_{pi} is $T_H + T_{RTS} + T_{CTS} + T_{DATA} + T_{ACK}$. T_H is preamble transmission time + PLCP header transmission time + MAC header transmission time. T_{DATA} is MSDU transmission time and T_{ACK} is ACK frame transmission time. T_{RTS} is RTS frame transmission time and T_{CTS} is CTS frame transmission time.

3. DCF throughput analysis

The back-off procedure of the DCF protocol is modeled as a discrete-time, two-dimensional Markov chain. Figure 6 shows the Bianchi's Markov chain model for the back-off window size [11]. We define $W = CW_{\min}$. Let m , the maximum back-off stage, be such value that $CW_{\max} = 2^m W$. We also define $w_i = 2^i W$, where $i \in (0, m)$ is called the back-off stage. Let $s(t)$ be the stochastic process representing the back-off stage $(0, \dots, m)$ of the station at time t . p is the probability that a transmission is collided or unsuccessfully executed.

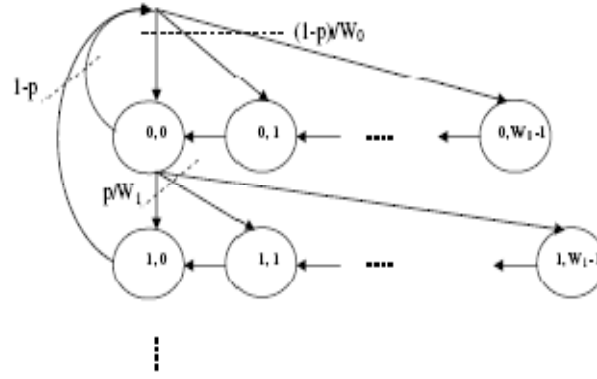


Figure 6. Markov chain model for the backoff window size

Table 5 shows physical and MAC layer parameters of IEEE 802.11a/g/n-based mobile LAN.

Parameter	Explanation
FER	Frame error rate
τ	Packet transmission probability
N	Number of stations
P	Payload size
T_{RTS}	RTS frame transmission time
T_{CTS}	CTS frame transmission time
T_H	PLCP preamble transmission time + PLCP header transmission time + MAC header transmission time
T_{DATA}	Payload transmission time
T_{ACK}	ACK frame transmission time
T_{BACK}	Block ACK frame transmission time
σ	Slot time
T_{SIFS}	SIFS time
T_{DIFS}	DIFS time
T_{EIFS}	EIFS time
CW_{min}	Minimum backoff window size
CW_{max}	Maximum backoff window size

We will present the analytical evaluation of saturation throughput with bit errors appearing in the transmitting channel. The number of stations n is assumed to be fixed and each station always has packets for transmission. In other words, we operate in saturation conditions, the transmission queue of each station is assumed to be always nonempty.

Let S be the normalized system throughput, defined as the fraction of time in which the channel is used to successfully transmit payload bits. P_{tr} is the probability that there is at least one transmission in the considered slot time. Since n stations contend on the channel and each transmits with probability τ , we get

$$P_{tr} = 1 - (1 - \tau)^n \quad (4)$$

A. 802.11a/g DCF throughput

Saturation throughput is represented as shown in (5).

$$\begin{aligned}
 S &= \frac{P_s P_{tr} P}{(1 - P_{tr})\sigma + P_{tr} P_s T_s + P_{tr} (1 - P_s) T_c} \\
 &= \frac{n\tau(1-\tau)^{n-1}(1-FER)P}{(1-\tau)^n\sigma + n\tau(1-\tau)^{n-1}(1-FER)T_s + [1-(1-\tau)^n]T_c - n\tau(1-\tau)^{n-1}(1-FER)T_c}
 \end{aligned} \tag{5}$$

P_s is the probability that a transmission successfully occurs on the channel and is given by the probability that exactly one station transmits on the channel, conditioned on the fact that at least one station transmits.

$$P_s = \frac{n\tau(1-\tau)^{n-1}(1-FER)}{P_{tr}} \tag{6}$$

The average amount of payload information successfully transmitted in a slot time is $P_{tr}P_sP$ since a successful transmission occurs in a slot time with probability $P_{tr}P_s$. The average length of a slot time is readily obtained considering that, with probability $1-P_{tr}$, the channel is empty, with probability $P_{tr}P_s$ it contains a successful transmission, and with probability $P_{tr}(1-P_s)$ it contains a collision. Where T_s is the average time the channel is sensed busy because of a successful transmission, and T_c is the average time the channel is sensed busy by each station during a collision or error. σ is the duration of an empty slot time. In the RTS/CTS access scheme, we obtain,

$$\begin{aligned}
 T_s &= T_{RTS} + T_{CTS} + T_{DATA} + T_{ACK} + T_{DIFS} + 3T_{SIFS} \\
 T_c &= T_{RTS} + T_{EIFS} = T_{RTS} + T_{SIFS} + T_{ACK} + T_{DIFS}
 \end{aligned} \tag{7}$$

B. 802.11n DCF throughput

In the uni-directional case shown in Fig. 5, the saturation throughput can be calculated as follows[12,13].

$$\begin{aligned}
 S &= \frac{E_p}{E_t} = \frac{L_p P_{tr} P_s (1 - P_e)}{T_{idle} P_{idle} + T_c P_{tr} (1 - P_s) + T_e P_{err} + T_{succ} P_{succ}} \\
 &= \frac{L_p n\tau(1-\tau)^{n-1}(1-P_e)}{(1-\tau)^n\sigma + n\tau(1-\tau)^{n-1}(1-P_e)T_{succ} + [1-(1-\tau)^n - n\tau(1-\tau)^{n-1}]T_c + n\tau(1-\tau)^{n-1}P_e T_e}
 \end{aligned} \tag{8}$$

where E_p is the number of payload information bits successfully transmitted in a virtual time slot, and E_t is the expected length of a virtual time slot. P_e is the error probability on condition that there is a successful RTS/CTS transmission in the time slot and can be defined as the FER (Frame Error Rate). P_{idle} is the probability of an idle slot. P_s is the probability for a non-collided transmission. P_{err} is the transmission failure probability due to error (no collisions but having transmission errors). P_{succ} is the probability for a successful transmission without collisions and transmission errors. T_{idle} , T_c and T_{succ} are the idle, collision and successful virtual time slot's length. T_e is the virtual time slot length for an error transmission sequence. L_p is the aggregated frame's payload length. In the RTS/CTS scheme, we obtain,

$$T_c = T_{RTS} + T_{EIFS} \quad (9)$$

$$T_{succ} = T_{RTS} + T_{CTS} + T_{DATA} + T_{BACK} + 3T_{SIFS} + T_{DIFS}$$

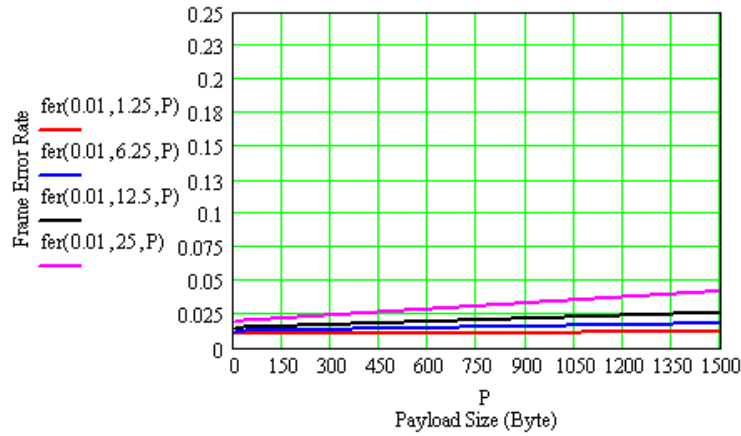
$$T_e = T_{RTS} + T_{CTS} + T_{DATA} + T_{EIFS} + 2T_{SIFS}$$

4. Numerical results

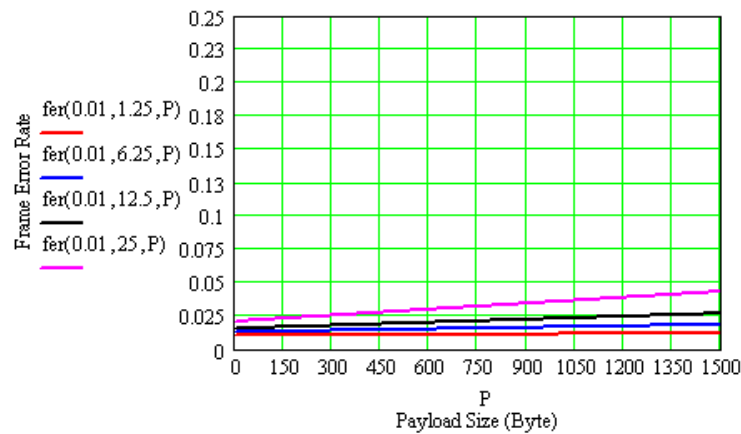
This section evaluated DCF throughput of the IEEE 802.11a/g-based mobile LAN with the maximum physical transmission rate of 54 Mbps and that of the IEEE 802.11n-based mobile LAN with the physical transmission rate of 130 Mbps considering 20 MHz MCS (modulation and coding scheme) parameters for two spatial streams, as shown in Figure 8. Out of the four different physical layers defined in the IEEE 802.11g standard, both ERP-OFDM and DSSS-OFDM standard are only used owing to their maximum transmission rate of 54 Mbps in this evaluation [14]. And the three common packets passed down to the MAC layer are 60 bytes (TCP ACK), 576 bytes (typical size for web browsing) and 1,500 bytes (the maximum size for Ethernet) in length. In the IEEE 802.11n-based mobile LAN, the number of packets aggregated in one MAC frame varies from 1 to 100, which leads to an aggregated frame's payload length (L_p) from 60, 576 and 1,500 bytes to 6, 57.6 and 150 Kbytes. In the Figure 7(a) ~ Figure 7(c), the symbol $fer(\rho, V, P)$ shows frame error rate of IEEE 802.11a/g. In the Figure 7(d), the symbol $fer(ns, \rho, V, P)$ shows frame error rate of IEEE 802.11n with the horizontal parameter of subframe' payload size. In the Figure 7(e), the symbol $fer(\rho, ns, V, P)$ shows frame error rate of IEEE 802.11n using the number of subframes as the horizontal parameter. It is generally identified that the higher mobile speed is, the higher fer is. In case of payload size, the same result mentioned above is also acquired. In the Figure 8(a) ~ Figure 8(c), the symbol $S(P, \rho, V, n, \tau)$ shows the saturation throughput over error-prone channel according to the number of stations(n) for common packet sizes (P) on the condition that packet transmission probability (τ), mobile velocity (V) and fading margin (ρ) are fixed. In the Figure 8(d) and Figure 8(e), the symbol $S(ns, P, \rho, V, n, \tau)$ and $S(P, ns, \rho, V, n, \tau)$ respectively shows the saturation throughput over error-prone channel according to the number of stations (n) and the typical number of packets aggregated in one MAC frame (ns) for two subframe length on the condition that packet transmission probability (τ), mobile velocity (V) and fading margin(ρ) are fixed. For example, in the Figure 8(a), if the number of stations is 7, packet transmission probability is 0.05, packet length is 1,500 and fading margin is 0.01, mobile station with the speed of 1.25 m/s can get the throughput of 27.238 Mbps, whereas mobile station with the speed of 25 m/s can get the throughput of 26.968 Mbps. In the Figure 8(d), if

subframe length is 30 and the same conditions mentioned above are applied, mobile station with the speed of 1.25 m/s can get the throughput of 113.511 Mbps with six stations, whereas mobile station with the speed of 25 m/s can get the throughput of 84.607 Mbps. Also, Figure 8(a ~ d) shows that the longer frame (or subframe) length is, the higher throughput is. And, for the same frame (or subframe) length, the higher speed is, the lower throughput is. As the results of evaluation, we also know that there is optimum number of stations to maximize saturation throughput under the error-prone channel. Specially, in Figure 8(e), the number of subframes is considered and it is identified that there is optimum number of subframes to maximize saturation throughput under the error-prone channel.

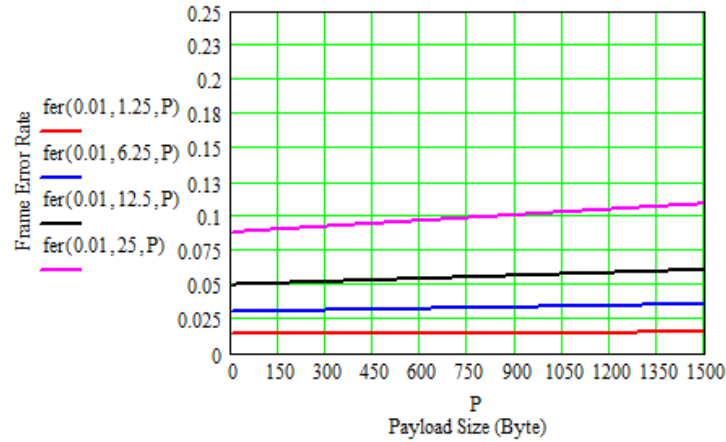
In conclusion, we obtained the fact that there exist an optimal number of stations (or subframes) to maximize the saturation throughput under the error-prone channel. Also, we can identify that the larger payload (or subpayload) size be, the higher saturation throughput be. And if a mobile velocity of station is increased, the throughput is decreased a little. Out of the three different physical layers defined in this analysis with the maximum transmission rate of 54 Mbps, which are IEEE 802.11g ERP-OFDM, IEEE 802.11g DSSS-OFDM and IEEE 802.11a OFDM, The DCF saturation throughput of IEEE 802.11a OFDM is the highest at all the channel environments. In the case of IEEE 802.11n, because A-MSDU (MAC Service Data Unit Aggregation) scheme is applied, it is identified that MAC efficiency of IEEE 802.11n is the best out of all four schemes.



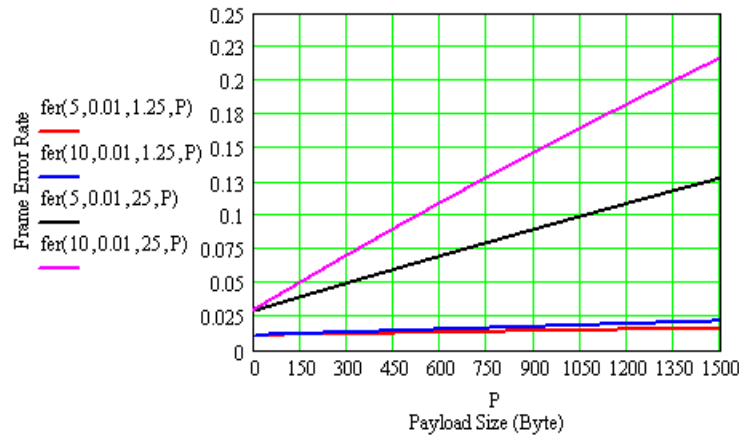
(a) 802.11a OFDM (54 Mbps)



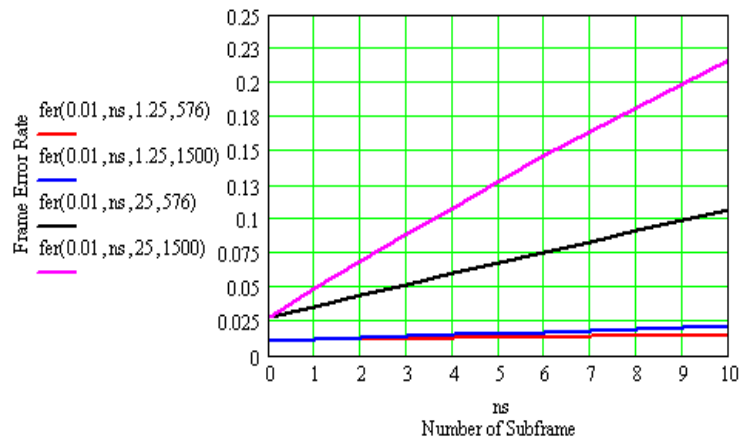
(b) 802.11g ERP-OFDM (54 Mbps)



(c) 802.11g DSSS-OFDM (54 Mbps)

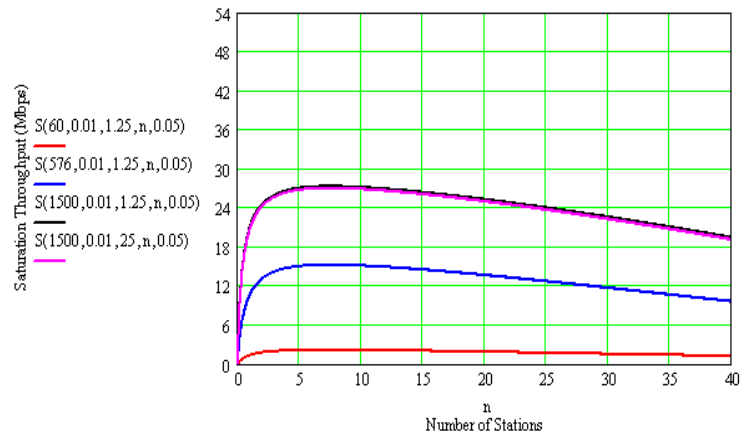


(d) 802.11n OFDM (58.5 Mbps, Payload size)

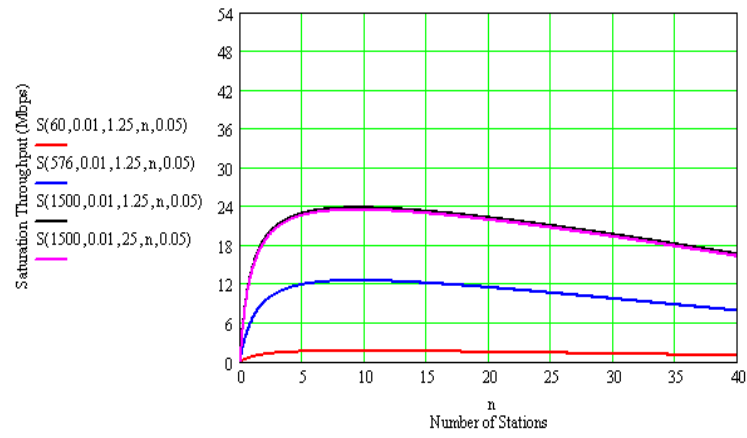


(e) 802.11n OFDM (58.5 Mbps, number of subframe)

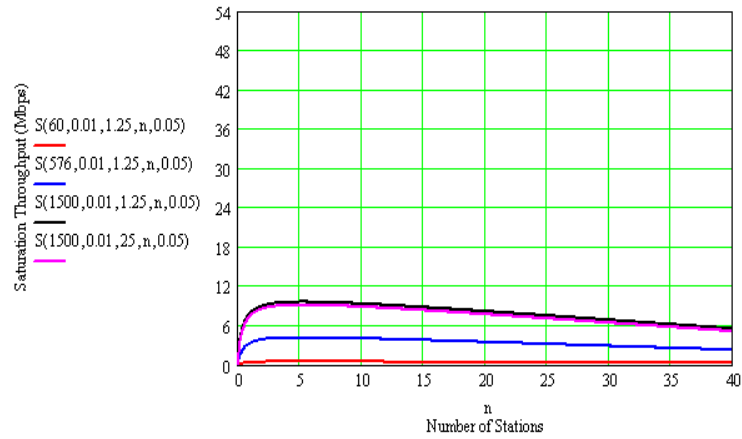
Figure 7. Frame error rate of IEEE 802.11a/g/n mobile LAN



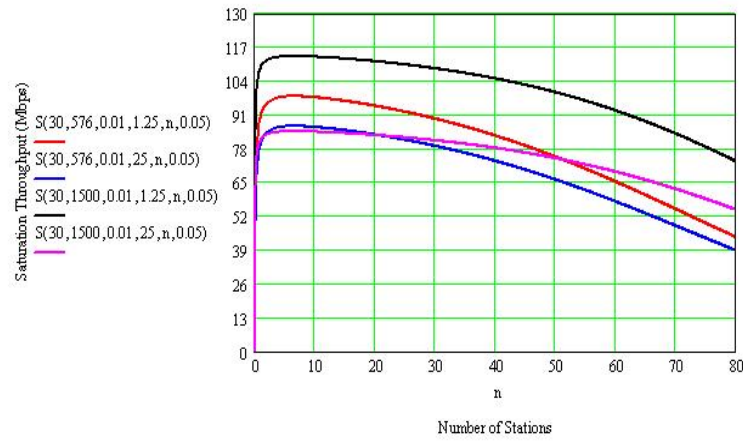
(a) 802.11a OFDM (54 Mbps)



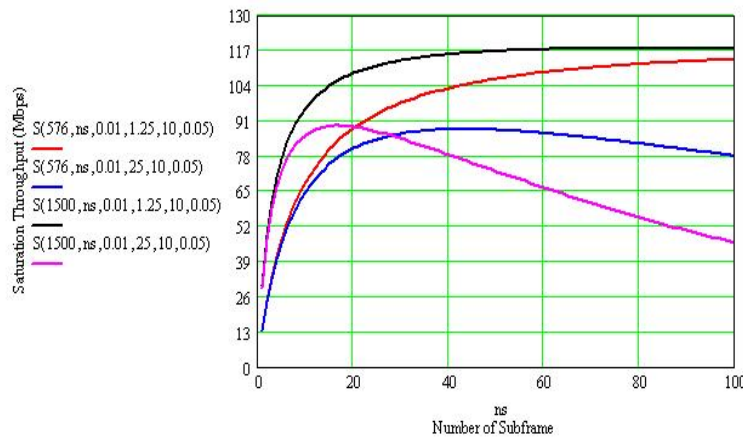
(b) 802.11g ERP-OFDM (54 Mbps)



(c) 802.11g DSSS-OFDM (54 Mbps)



(d) 802.11n OFDM (130 Mbps, number of stations)



(e) 802.11n OFDM (130 Mbps, number of subframe)

Figure 8. DCF throughput of IEEE 802.11a/g/n mobile LAN

Conclusions

This paper explored the saturation throughput performance of DCF protocol in the IEEE 802.11a/g/n-based mobile LAN under the error-prone channel. IEEE 802.11a and IEEE 802.11g have the same maximum transmission rate of 54 Mbps, but the DCF saturation throughput of IEEE 802.11a is higher than that of IEEE 802.11g. Of the two 802.11g standards, DCF saturation throughput of IEEE 802.11g ERP-OFDM is higher than that of IEEE 802.11g DSSS-OFDM. We are recognizing that a IEEE 802.11n-based device can operate with a IEEE 802.11 legacy devices, but IEEE 802.11a-based device does not operate with a IEEE 802.11b/g-based device. So this interoperability have to be considered for designing and constructing IEEE 802.11a/g/n-based mobile LAN.

References

- [1] Upkar Varshney, "The Status and Future of 802.11-based Wireless LANs," *IEEE Computer*, Jun. 2003, pp. 102-105.
- [2] C. Siva Ram Murthy and B. S. Manoj, "Ad Hoc Wireless Networks," Prentice Hall, 2004, pp. 172-179.

- [3] Carlos de Morais Cordeiro and Dharma Prakash Agrawal, "Ad Hoc & Sensor Networks," World Scientific, 2006, pp. 172-187.
- [4] Zuoyin Tang, Zongkai Yang, Jianhua He and Yanwei Liu, "Impact of Bit Errors on the Performance of DCF for Wireless LAN," *IEEE*, pp. 529-533, 2002.
- [5] Dimitris Vassiss, George Kormentzas, Angelos Rouskas and Ilias Maglogiannis, "The IEEE 802.11g Standard for High data rate WLANs," *IEEE Network*, pp. 21-26, May/June, 2005.
- [6] Nghia T. Dao and Robert A. Malaney, "Throughput Performance of Saturated 802.11g Networks," *AusWireless 2007*, 2007.
- [7] Xi Yong, Wei Ji Bo and Zhuang Zhao Wen, "Throughput Analysis of IEEE 802.11 DCF over Correlated Fading Channel in MANET," *IEEE*, pp. 694-697, 2005
- [8] IEEE 802.11b, "Part 11: Wireless LAN Medium Access Control (MAC) and Physical Layer (PHY) Specification: High-Speed Physical Layer Extension in the 2.4 GHz Band," 1999.
- [9] IEEE Std 802.11n 2009 "Part 11: Wireless LAN Medium Access Control(MAC) and Physical Layer (PHY) specifications: Enhancements for Higher Throughput," Oct. 2009.
- [10] D. Skordoulis, Q. Ni, H. Chen, A. P. Stephens, C. Liu and A. Jamalipour, "IEEE 802.11n MAC Frame Aggregation Mechanisms for Next-Generation High-Throughput WLANs," *IEEE Wireless Communications*, vol. 15, pp.40-47, Feb.2008.
- [11] Giuseppe Bianchi, "Performance Analysis of the IEEE 802.11 Distributed Coordination Function," *IEEE Journal on Selected Areas in Communications*, Vol. 18, No.3, pp. 535-547, March 2000.
- [12] F. Zheng and J. Nelson, "Adaptive Design for the Packet Length of IEEE 802.11n Networks," in *2008 IEEE Intern. Conf. Communications*, Beijing, May.2008, pp. 2490-2495.
- [13] Y. Lin and V. W. S. Wong, "Frame Aggregation and Optimal Frame Size Adaptation for IEEE 802.11n WLANs," in *Proc. IEEE GLOBECOM*, San Francisco, CA, Nov. 2006, pp. 1-6.
- [14] Ha Cheol Lee, "A MAC Layer Throughput over Error-Free and Error-Prone Channel in The 802.11a/g-based Mobile LAN," *MICC 2009*, Dec. 2009



Ha Cheol Lee was born in Korea in 1960. He received B.E., M.E. and Ph. D. from The Department of Information and Communication Engineering, Korea Aerospace University, Korea in 1983, 1990 and 1999 respectively. He is working as professor in Dept. of Information and Communication Eng. of Yuhan University in Korea since 1995. He was a research engineer in ETRI (Electronic Telecommunication Research Institute) and KT (Korea Telecom) from 1983 to 1995 in Korea. He also acquired certificate of professional engineer in 1993 in Korea. His areas of interest are wireless LAN, Home network and PAN design.